

# Field-induced Single-ion magnetic behaviour in a highly luminescent Er<sup>3+</sup> complex

J.T. Coutinho<sup>a</sup>, L.C.J. Pereira<sup>a\*</sup>, P. Martín-Ramos<sup>b,c</sup>, M. Ramos Silva<sup>b</sup>, Y.X. Zheng<sup>d</sup>, X. Liang<sup>d</sup>, H.Q. Ye<sup>e</sup>, Y. Peng<sup>f</sup>, P.J. Baker<sup>e</sup>, P.B. Wyatt<sup>f</sup> and W.P. Gillin<sup>e,g</sup>

<sup>a</sup> Solid State Group, UCQR, IST/CTN, Instituto Superior Técnico, UTL, Estrada Nacional 10, km 139.7, 2695-066 Bobadela LRS, Portugal. E-mail: [lpereira@ctn.ist.utl.pt](mailto:lpereira@ctn.ist.utl.pt). Phone: 00351219946259.

<sup>b</sup> CEMDRX, Physics Department, Universidade de Coimbra, Rua Larga, P-3004-516 Coimbra, Portugal.

<sup>c</sup> Advanced Materials Laboratory, ETSIIAA, Universidad de Valladolid, Avenida de Madrid 44, 34004 Palencia, Spain.

<sup>d</sup> State Key Laboratory of Coordination Chemistry, Nanjing National Laboratory of Microstructures, School of Chemistry and Chemical Engineering, Nanjing University, Nanjing 210093, China

<sup>e</sup> Materials Research Institute and School of Physics and Astronomy Queen Mary University of London, Mile End Road, London E1 4NS, UK

<sup>f</sup> Materials Research Institute and School of Biological and Chemical, Sciences, Queen Mary University of London, Mile End Road, London E1 4NS, UK

<sup>g</sup> College of Physical Science and Technology, Sichuan University, Chengdu 610064, China.

## Abstract

The magnetic properties of a perfluorinated Er<sup>3+</sup> complex, with record luminescent properties, have been investigated. [Er(F-TPIP)<sub>3</sub>] displays thermally activated slow relaxation of the magnetisation under an applied H<sub>DC</sub> field of 500 Oe. The effective relaxation barrier E<sub>eff</sub> is found to be 26.8 K (18.6 cm<sup>-1</sup>). At zero static field, efficient quantum tunnelling of the magnetization occurs.

## Highlights

- Under DC field, slow relaxation of magnetisation occurs with barrier of 27 K
- Efficient quantum tunneling of magnetization is displayed at zero static field
- The lifetime value of the <sup>4</sup>I<sub>13/2</sub> multiplet is τ=0.22 ms
- [Er(F-TPIP)<sub>3</sub>] complex can be considered a multifunctional material

**Keywords:** Luminescence; Magnetic properties; Optical materials; Powder diffraction.

## 1. Introduction

Lanthanide elements have unique properties readily explained by the electronic configuration of these atoms and their derived ions, which commonly exist in their trivalent state in aqueous solutions and in many complexes. The shielding of the 4f orbitals by the filled 5p<sup>6</sup> subshells results in singular spectroscopic properties: 4f–4f absorption bands are parity-forbidden, with very low molar absorption coefficients, and there is a characteristic line-like emission (leading to high colour purity) in the visible and/or near infrared ranges. Due to electric dipole selection rules, direct excitation of the Ln<sup>3+</sup> ions seldom yields good luminescent materials. Indirect excitation (referred to as *sensitization* or *antenna effect*) has been suggested as a way to overcome this. The common approach has been to coordinate the lanthanide ion with an organic ligand and ultraviolet to visible light is absorbed by the coordinating organic ligands and the energy is transferred to the trivalent ion, which re-emits it at a longer wavelength. The Er<sup>3+</sup> ion, specifically, emits at a wavelength of 1.53 μm, at the low-loss window of silica fibres. The use of the antenna effect in such cases has been hampered by the quenching of the infrared emission of Er<sup>3+</sup> ion by the C-H or O-H oscillators present in most organic ligand molecules. A possible

strategy to overcome such drawback is the substitution of the H atoms with heavier halogen atoms in the ligands. Successful examples showing the improvement of the NIR light emission have been reported in the literature [1-3].

The compound studied in this paper is one of such compounds: a  $\text{Er}^{3+}$  complex with a bidentate chelating ligand, the tetrakis(pentafluorophenyl)imidodiphosphinate (Figure 1). This complex has shown to exhibit an intrinsic radiative lifetime of  $13 \pm 1$  ms.

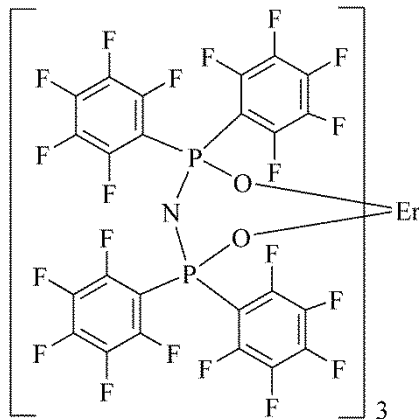


**Figure 1.** Chemical structure of Erbium-*tris*(tetra-pentafluorophenylimidodiphosphinate),  $[\text{Er}(\text{F-TPIP})_3]$ .

When this compound,  $[\text{Er}(\text{F-TPIP})_3]$ , is associated with a perfluorinated zinc-based organic chromophore, the zinc salt of 2-(3,4,5,6-tetrafluoro-2-hydroxyphenyl)-4,5,6,7-tetrafluorobenzothiazole,  $[\text{Zn}(\text{F-BTZ})_2]$  [4], in a composite material, it becomes very highly sensitised. In this situation the sensitization is attained in an indirect way: the  $[\text{Zn}(\text{F-BTZ})_2]$  in the medium is able to absorb radiation in the 350 to 475 nm range and transmit the energy to the erbium ion in the  $[\text{Er}(\text{F-TPIP})_3]$ . In this environment the Er has a lifetime of  $\sim 0.86$  ms which indicating a quantum efficiency of  $\sim 7\%$ , the highest ever reported for erbium in a coordination compound.

Even more important from the technological point of view is that such composite may be electrically stimulated, in a OLED structure, yielding significant emission from erbium(III) [5].

Lanthanides complexes are also promising materials in the field of Single-Molecule Magnetism or Single-Ion Magnetism. In SMMs and SIMs, an anisotropy barrier obstructs the reversal of the molecular magnetic moment at very low temperatures. In these conditions, individual molecules/complexes can display a memory effect, thus posing new possibilities for high-density information storage and processing through single moment manipulation [6,7].

The current approach to obtain SIMs with high anisotropy barriers and high blocking temperatures involves replacing large clusters of  $3d$  metals with lanthanide complexes [8,9]. The unquenched angular momentum of the lanthanides ensures intrinsic magnetic anisotropy and large magnetic moments, and a thermal energy barrier up to 915 K has been reported for a terbium(III) bis-phthalocyaninato complex [10].

There are some examples of lanthanide complexes where both luminescent emission and slow relaxation of the magnetization occur [11-18]. This configures these materials as multifunctional materials. Such materials have an increased value: they may provide a correlation between photoluminescence, static susceptibilities and dynamic magnetic relaxation. The measurement of the energy gap between the ground and excited states by two independent techniques may reveal if the magnetisation reversal is achieved through the first excited state or through higher excited states, a hypothesis only recently raised [19,20].

These multifunctional materials may also find an application in Quantum Computing. Scientists are probing SIMs as qubits (the processing elements in quantum computers) since they

are easier to manipulate than atomic-sized objects (their magnetic moments have an order of magnitude larger than the moment of an electron), but still their quantum behavior reflects atomic-scale objects rather than macroscopic ones. To implement the quantum algorithms, scientists have to create and control superposition of states. The magnetic fields can be used to tune the barrier height and prevent or promote quantum tunneling between the lanthanide magnetic states. Moreover, for these multifunctional materials, radiation can also be used to influence the magnetic state. Therefore the large QE presented by these materials therefore make them particularly impressive candidate molecules for quantum computing applications. Previous work has shown that the exposure of the molecules to x-rays accelerates the relaxation of magnetization in a Dy<sup>3+</sup> based SIM [21]. The demagnetization upon photo-excitation has also been reported for a 3d–4f hybrid SMMs based on Cu<sup>2+</sup> and Dy<sup>3+</sup> ions [22].

## 2. Experimental section

### 2.1. Physical and spectroscopic measurements

Differential scanning calorimetry (DSC) data were obtained on a DSC TA instrument model Q100 v.9.0 with a heating rate of 10°C/min under a N<sub>2</sub> atmosphere.

The powder diffractogram was obtained using an ENRAF-NONIUS FR590 powder diffractometer equipped with an INEL120 detector (Debye-Scherrer geometry). The powder was used to fill a glass capillary, which was slowly rotating upon data collection.

The photoluminescence spectrum of the complex was obtained for the sample in powder form upon excitation at 385nm using an electrically modulated semiconductor diode laser modulated at 123Hz. Luminescence was focused and filtered onto the adjustable entrance slits of a Jobin Yvon Horiba Triax 550 spectrometer and detected using a Hamamatsu R5509-72 liquid nitrogen-cooled detector. Signals were measured using a 7265 DSP Perkin Elmer lock-in amplifier and recorded with the resolution of 2 nm. Lifetime data were recorded at the peak of the photoluminescence spectra (1542 nm) at 300 K using the ~7 ns pulses (at a wavelength of 520nm) from a Continuum Panther optical parametric oscillator (OPO) pumped by a Surelite (SLI-10) Nd:YAG laser.. Lifetime data were fitted with a single-exponential decay model using a Marquardt–Levenberg algorithm to find the best fit.

### 2.2. Magnetic measurements

The magnetic susceptibility under several magnetic fields was measured with a S700X SQUID magnetometer (Cryogenic Ltd) in the temperature range 4-300K and assuming a diamagnetic contribution of  $-6.160 \times 10^{-4}$  emu/mol (estimated from tabulated Pascal constants). Field dependence of the magnetization was measured up to 5 T at different fixed temperatures from 1.6 K to 10 K. AC measurements were taken using a MagLab 2000 system (Oxford Instruments) with a AC field of 5 Oe. Temperature dependence of AC magnetic susceptibility was measured in the 10-10000 Hz frequency range under a zero and a 500 Oe static DC field. Additional isothermal AC susceptibility measurements,  $\chi_{AC}=f(\omega)$ , were taken in the 10-10000 Hz frequency range, between 1.6 and 7 K.

## 3. Results and discussion

### 3.1. X-ray powder diffraction

Figure 2 shows the experimental diffraction pattern of the complex and the simulated powder pattern from the single crystal structure using PLATON [23]. There is an excellent match between the simulated and the experimental diffractograms: the peaks appear at the predicted theta angles at the same relative intensities. The experimental diffractogram shows a background higher for low theta angles as expected from the diffuse scattering of X-Rays by glass and air, a common characteristic when using rotating capillaries in a Debye-Scherrer geometry. Powder diffraction

shows that all the material synthesized in crystalline form corresponds to the same structure as the small single crystals reported for single-crystal X-ray diffraction by Ye *et al.* [24].

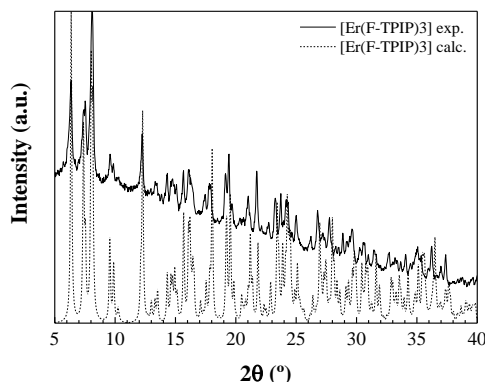


**Figure 2.** Experimental versus calculated X-ray powder patterns for [Er(F-TPIP)<sub>3</sub>]

### 3.2. Thermal analysis by DSC

Probably due to the high binding energy of O=P and N=P bonds in the F-TPIP ligands, the [Er(F-TPIP)<sub>3</sub>] complex shows an extraordinary stability: the DSC curve (Figure 3) shows only an endothermic effect at 311.2 °C, which can be attributed to melting. No signs of decomposition are observed up to 350 °C. This is in agreement with the TG/DTG data reported by Zheng *et al.* for the analogous Eu<sup>3+</sup> complex [25], in which no weight loss was observed until the decomposition of the ligands at about 420 °C.

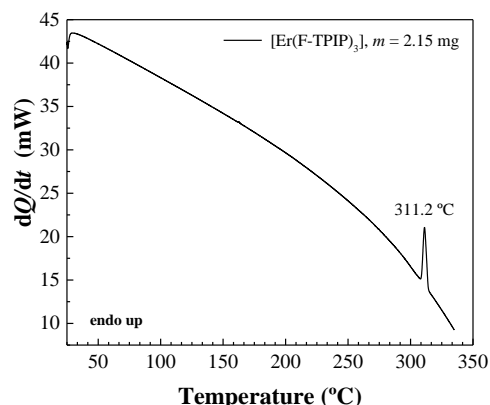


**Figure 3.** DSC curve of [Er(F-TPIP)<sub>3</sub>] complex

### 3.3. Luminescence

The infrared photoluminescence spectrum of the material upon excitation at 520 nm is depicted in Figure 4(a), and is in good agreement with that reported by Mancino *et al.* [26]. It is worth noting that the Er<sup>3+</sup> emission observed for the [Er(F-TPIP)<sub>3</sub>] complex is sharp and shows distinct fine structure, which is in contrast to many reported emission spectra of other erbium chelates.

The PL decay of the <sup>4</sup>I<sub>13/2</sub> multiplet is shown in Figure 4(b). The obtained lifetime decay is best fitted with a dual exponential fit which gives a major lifetime of 0.279 ms which is in agreement with the values expected for bulk powder [26], but it can be improved up to 0.86 ms [5] by diluting the complexes in order to minimize ion-ion interactions. Such dilution approaches the conditions in which [Er(F-TPIP)<sub>3</sub>] samples would be prepared for usage in quantum computing [12,27].

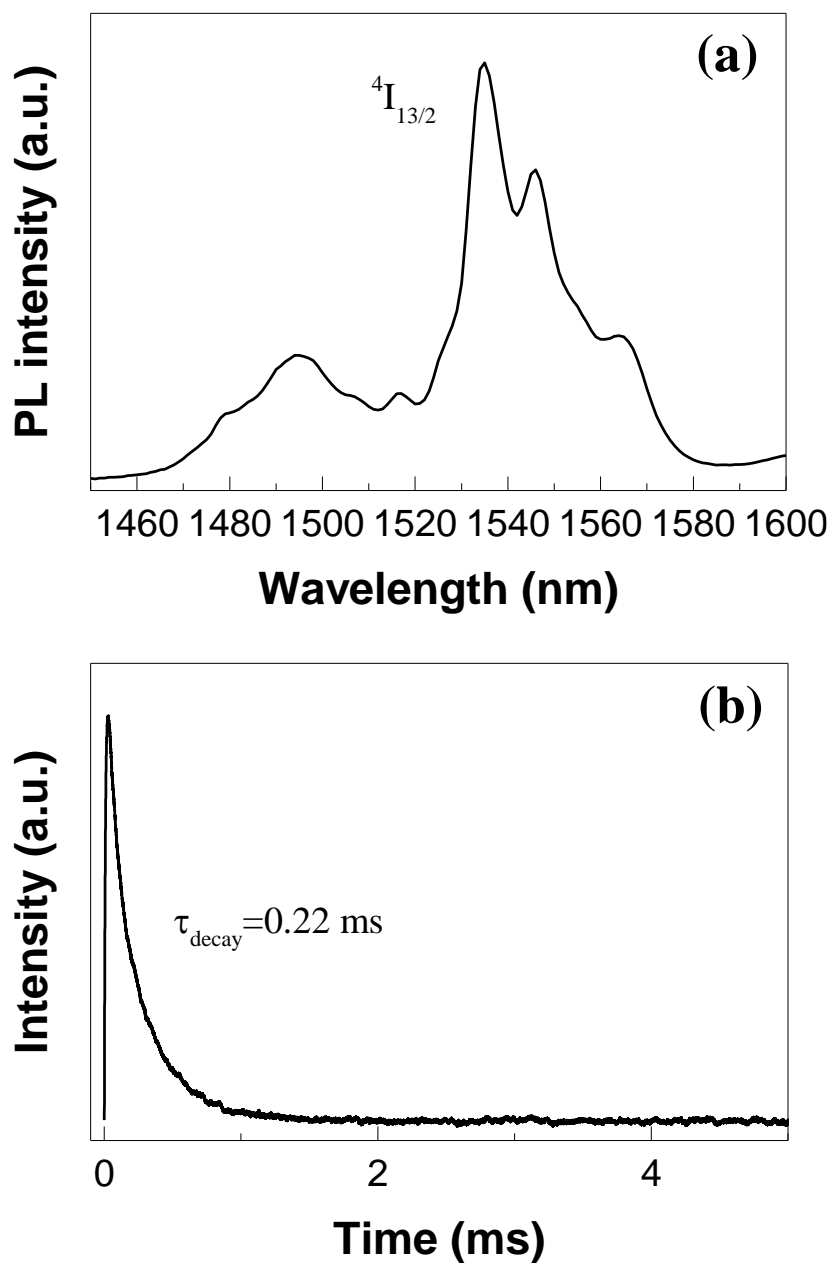


**Figure 4.** (a) PL spectrum and (b) luminescence decay profile of [Er(F-TPIP)<sub>3</sub>] in powder form.

### 3.4. Magnetic measurements

As seen in Figure 5, the room temperature  $\mu_{\text{eff}}$  value of [Er(F-TPIP)<sub>3</sub>],  $\mu_{\text{eff}}(300\text{K}) = 9.267 \mu_{\text{B}}$ , is close to the expected value of  $9.6 \mu_{\text{B}}$  for a non-interacting Er<sup>3+</sup> ion ( ${}^4I_{15/2}$ , and  $g = 6/5$ ). A gradual decrease of  $\mu_{\text{eff}}$  upon cooling can be understood as resulting from a progressive depopulation of excited Stark sublevels due to the ligand field, suggesting the presence of significant magnetic anisotropy as commonly observed in lanthanide compounds.

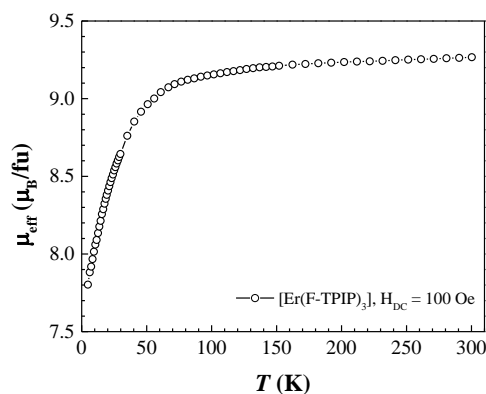


**Figure 5.** Static magnetic properties of the  $[\text{Er}(\text{F-TPIP})_3]$  complex: plot of  $\mu_{\text{eff}}$  in the 4.8-300 K range and  $H_{\text{DC}}=100$  Oe.

The magnetic field dependences of magnetization at several temperatures, measured up to 5 T (up to 10 T at 1.6 K) with a sweeping rate of  $90 \text{ Oe}\cdot\text{s}^{-1}$ , are shown in Figure 6a. At 1.6 K a clear opening of the magnetic hysteresis is observed as one moves away from zero field, revealing strong field dependence. The absence of coercivity can be due to an efficient quantum tunnelling of the magnetization occurring at zero field, probably caused by low symmetry components of the crystal field, as it was already observed in other mononuclear lanthanide [17,18,28] and uranium [29,30] compounds with SMM behaviour. At this temperature and up to 10 T, magnetization approaches a value of  $7.9 \mu_{\text{B}}$ , still far from the expected saturation value for a free  $\text{Er}^{3+}$  ion. This fact can be explained by the magnetic anisotropy of the compound, which is further confirmed by the non-superimposition of the  $M$  vs.  $B/T$  curves at lower temperatures (Figure 6b).

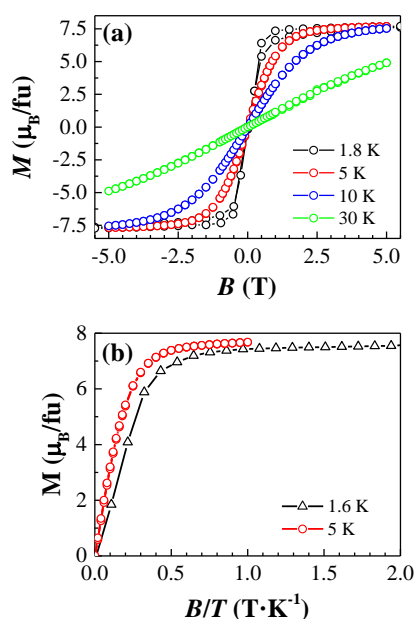


**Figure 6.** (a) Hysteresis loops at different temperatures for  $[\text{Er}(\text{F-TPIP})_3]$  with a sweeping rate of  $90 \text{ Oe}\cdot\text{s}^{-1}$ ; (b) reduced magnetization plots for  $[\text{Er}(\text{F-TPIP})_3]$  at 1.6 and 5 K.

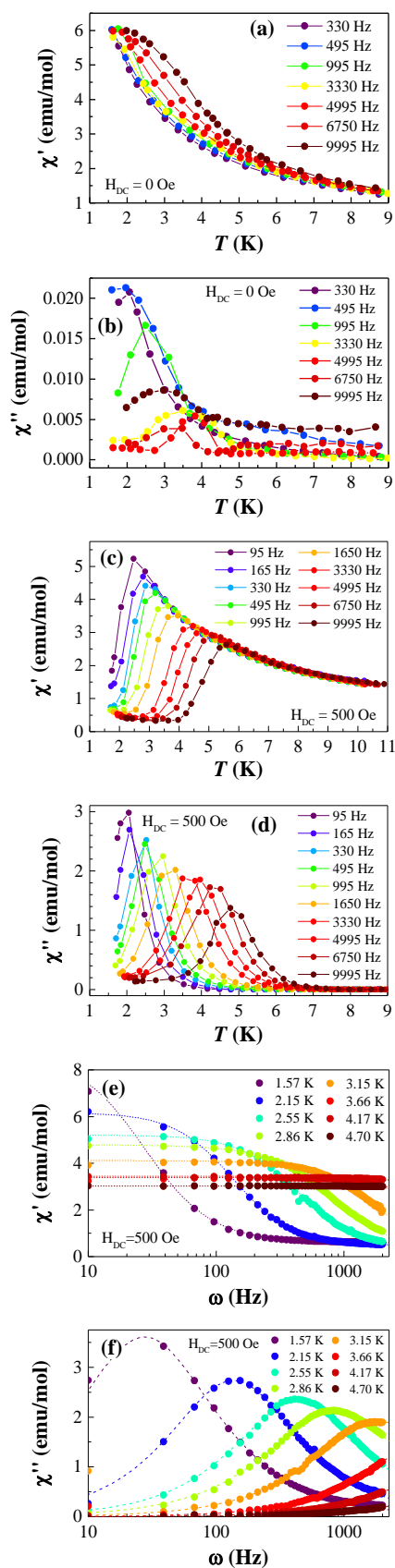
Clear evidence for slow relaxation of the magnetisation is also given by measuring the AC susceptibility components,  $\chi'$  and  $\chi''$ , at fixed frequencies in the low temperature range, 1.6-10 K. In a similar fashion to what was observed in other  $\text{Er}^{3+}$  complexes classified as SIMs [17], under zero DC field the in-phase component,  $\chi'$ , was found to be almost frequency independent, while the out-of-phase component,  $\chi''$ , presents a small frequency dependence with a local maximum shifting to higher temperatures as frequency increases (Figure 7a). The application of a small static magnetic field of 500 Oe drastically changes the relaxation dynamics with the occurrence

of peaks in both  $\chi'$  and  $\chi''$  components, that which show strong frequency and temperature dependence (Figure 7b and Figure 7c). This behavior denotes the presence of a fast zero-field tunneling of the magnetization between sub-levels, which is suppressed with the application of the DC field.

The magnetization relaxation rate was probed in the temperature range 1.6 to 6 K by measuring  $\chi'$  and  $\chi''$ , at fixed temperatures while the frequency,  $\omega$ , of the AC field was varied from 10 Hz to 10 kHz. These data provided Cole-Cole plots ( $\chi''$  vs.  $\chi'$  plots) for those different temperatures that were fitted with the generalized Debye model [31,32],  $\chi(\omega) = \chi_S + (\chi_T + \chi_S)/(1 + i\omega\tau)^{1-\alpha}$ , where  $\chi_S$  and  $\chi_T$  are the adiabatic and isothermal susceptibilities,  $\tau$  is the average magnetization relaxation time, and  $\alpha$  is a parameter ranging from 0 to 1 which quantifies the width of the relaxation time distribution ( $\alpha = 0$  corresponds to the ideal Debye model, with a single relaxation time). Figure 8a) shows the Cole-Cole plots obtained under a DC field of 500 Oe. The small  $\alpha$  values obtained (see

Table 1), along with the nearly semi-circular and symmetrical shape of the Cole-Cole plots, support the existence of a single relaxation process.

When plotted with the correspondent inverse of temperature, these single relaxation times  $\tau$  have an activated temperature dependency (Figure 8b) that follows an Arrhenius law,  $\tau(T) = \tau_0 \cdot \exp(E_{\text{eff}}/k_B T)$  in the higher temperature range (dashed line), with a pre-exponential factor  $\tau_0 = 1.73 \times 10^{-8}$  s and an effective relaxation barrier of  $E_{\text{eff}} = 26.8$  K ( $18.6 \text{ cm}^{-1}$ ) which are within the range of most of other well-known *d*- [33,34] and *f*-element SMMs [17,18,35]. In the lower temperature range, a clear deviation from this activated regime is noticed, likely due to the approaching of a quantum tunnelling regime expected to occur at lower temperatures.

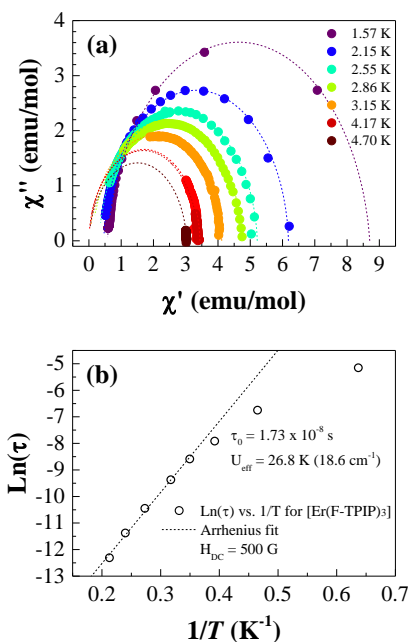


**Figure 7.** Temperature and frequency dependences of the AC susceptibility at different static fields,  $H_{DC}=0$  Oe and  $H_{DC}=500$  Oe, for [Er(F-TPIP)<sub>3</sub>] complex. In figures (e) and (f) Debye fittings are shown as dashed lines.  $H_{AC}=5$  Oe in all cases.



**Table 1.** Debye model fitting parameters from 1.6 to 4.8 K for [Er(F-TPIP)<sub>3</sub>].

T (K)	$\chi_s$ (emu/mol)	$\chi_T$ (emu/mol)	$\alpha$	$\tau$ (s <sup>-1</sup> )
1.57	0.574	8.703	0.076	5.780E-03
2.15	0.462	6.182	0.029	1.170E-03
2.55	0.323	5.216	0.034	3.654E-04
2.86	0.100	4.728	0.067	1.821E-04
3.15	0.024	4.116	0.042	8.526E-05
3.66	0.000	3.440	0.023	2.905E-05
4.17	0.000	3.386	0.020	1.146E-05
4.70	0.000	3.026	0.043	4.513E-06

**Figure 8.** (a) Argand diagrams and Debye fittings; (b) Arrhenius Law fitting for [Er(F-TPIP)<sub>3</sub>] complex.  $H_{AC}=5$  Oe;  $H_{DC}=500$  Oe.

## 4. Conclusions

We have shown that a perfluorinated Er<sup>3+</sup> complex, [Er(F-TPIP)<sub>3</sub>], displays slow magnetic behavior. Although AC susceptibility measurements indicate the presence of significantly fast quantum tunneling magnetization at zero static field, as evidenced by the absence of coercivity at very low temperatures, the application of a static field slows down the relaxation and an energy barrier for the moment reversal can be identified.

The high photoluminescence efficiency allows 100% population inversion in a single crystal, and a controlled radiative decay to the <sup>4</sup>I<sub>15/2</sub> multiplet may provide a precise proportion of spin states useful for quantum computing.

This compound is therefore a multifunctional material, combining record luminescent properties with field-induced SIM behavior.

## Acknowledgements

J.T.C. acknowledges the support by Fundação para a Ciência e a Tecnologia (FCT) under the scholarship SFRH/BD/84628/ 2012. P.M.-R. would like to thank Iberdrola Foundation for their financial support. CEMDRX group acknowledges funds from FEDER (Programa Operacional Factores de Competitividade COMPETE) and from FCT-Fundação para a Ciência e

a Tecnologia under the Project PEst-C/FIS/UI0036/2014. W.P.G. acknowledges financial support from EPSRC (EP/K004484/1).

## References

- [1] R. Van Deun, P. Fias, P. Nockemann, A. Schepers, T.N. Parac-Vogt, K. Van Hecke, L. Van Meervelt, K. Binnemans, Rare-Earth Quinolinates: Infrared-Emitting Molecular Materials with a Rich Structural Chemistry, *Inorg. Chem.*, 43 (2004) 8461-8469.
- [2] J. Gordon, J. Ballato, D.W. Smith Jr, J. Jin, Optical properties of perfluorocyclobutyl polymers. III. Spectroscopic characterization of rare-earth-doped perfluorocyclobutyl polymers, *J. Opt. Soc. Am. B*, 22 (2005) 1654.
- [3] P.B. Glover, A.P. Bassett, P. Nockemann, B.M. Kariuki, R. Van Deun, Z. Pikramenou, Fully Fluorinated Imidodiphosphate Shells for Visible- and NIR-Emitting Lanthanides: Hitherto Unexpected Effects of Sensitizer Fluorination on Lanthanide Emission Properties, *Chem. Eur. J.*, 13 (2007) 6308-6320.
- [4] Z. Li, A. Dellali, J. Malik, M. Motevalli, R.M. Nix, T. Olukoya, Y. Peng, H. Ye, W.P. Gillin, I. Hernández, P.B. Wyatt, Luminescent Zinc(II) Complexes of Fluorinated Benzothiazol-2-yl Substituted Phenoxide and Enolate Ligands, *Inorg. Chem.*, 52 (2013) 1379-1387.
- [5] H.Q. Ye, Z. Li, Y. Peng, C.C. Wang, T.Y. Li, Y.X. Zheng, A. Sapelkin, G. Adamopoulos, I. Hernández, P.B. Wyatt, W.P. Gillin, Organo-erbium systems for optical amplification at telecommunications wavelengths, *Nature Mater.*, 13 (2014) 382-386.
- [6] L. Bogani, W. Wernsdorfer, Molecular spintronics using single-molecule magnets, *Nature Mater.*, 7 (2008) 179-186.
- [7] S.-D. Jiang, B.-W. Wang, H.-L. Sun, Z.-M. Wang, S. Gao, An Organometallic Single-Ion Magnet, *J. Am. Chem. Soc.*, 133 (2011) 4730-4733.
- [8] E. Ruiz, J. Cirera, J. Cano, S. Alvarez, C. Loose, J. Kortus, Can large magnetic anisotropy and high spin really coexist?, *Chem. Commun.*, (2008) 52.
- [9] B.W. Wang, X.Y. Wang, H.L. Sun, S.D. Jiang, S. Gao, Evolvement of molecular nanomagnets in China, *Philosophical Transactions of the Royal Society A: Mathematical, Physical and Engineering Sciences*, 371 (2013) 20120316-20120316.
- [10] F. Branzoli, P. Carretta, M. Filibian, G. Zoppellaro, M.J. Graf, J.R. Galan-Mascaros, O. Fuhr, S. Brink, M. Ruben, Spin Dynamics in the Negatively Charged Terbium (III) Bis-phthalocyaninato Complex, *J. Am. Chem. Soc.*, 131 (2009) 4387-4396.
- [11] S. Mohapatra, B. Rajeswaran, A. Chakraborty, A. Sundaresan, T.K. Maji, Bimodal Magneto-Luminescent Dysprosium (DyIII)-Potassium (K)-Oxalate Framework: Magnetic Switchability with High Anisotropic Barrier and Solvent Sensing, *Chem. Mater.*, 25 (2013) 1673-1679.
- [12] J. Ruiz, A.J. Mota, A. Rodríguez-Diéguez, S. Titos, J.M. Herrera, E. Ruiz, E. Cremades, J.P. Costes, E. Colacio, Field and dilution effects on the slow relaxation of a luminescent DyO9 low-symmetry single-ion magnet, *Chem. Commun.*, 48 (2012) 7916.
- [13] M. Fang, J.-J. Li, P.-F. Shi, B. Zhao, P. Cheng, Structures, luminescence, and slow magnetic relaxation of eight 3D lanthanide-organic frameworks, *Dalton Trans.*, 42 (2013) 6553.
- [14] Y.-L. Hou, G. Xiong, B. Shen, B. Zhao, Z. Chen, J.-Z. Cui, Structures, luminescent and magnetic properties of six lanthanide-organic frameworks: observation of slow magnetic relaxation behavior in the DyIII compound, *Dalton Trans.*, 42 (2013) 3587.
- [15] J. Long, R. Vallat, R.A.S. Ferreira, L.D. Carlos, F.A. Almeida Paz, Y. Guari, J. Larionova, A bifunctional luminescent single-ion magnet: towards correlation between luminescence studies and magnetic slow relaxation processes, *Chem. Commun.*, 48 (2012) 9974.
- [16] G. Cucinotta, M. Perfetti, J. Luzon, M. Etienne, P.-E. Car, A. Caneschi, G. Calvez, K. Bernot, R. Sessoli, Magnetic Anisotropy in a Dysprosium/DOTA Single-Molecule Magnet: Beyond Simple Magneto-Structural Correlations, *Angew. Chem. Int. Ed.*, 51 (2012) 1606-1610.
- [17] P. Martín-Ramos, M. Ramos Silva, J.T. Coutinho, L.C.J. Pereira, P. Chamorro-Posada, J. Martín-Gil, Single-Ion Magnetism in a Luminescent Er<sup>3+</sup>  $\beta$ -Diketonato Complex with Multiple Relaxation Mechanisms, *Eur. J. Inorg. Chem.*, 2014 (2014) 511-517.

- [18] M. Ramos Silva, P. Martín-Ramos, J.T. Coutinho, L.C.J. Pereira, J. Martín-Gil, Effect of the capping ligand on luminescent erbium(III)  $\beta$ -diketonate single-ion magnets, *Dalton Trans.*, 43 (2014) 6752-6761.
- [19] Y.-N. Guo, L. Ungur, G.E. Granroth, A.K. Powell, C. Wu, S.E. Nagler, J. Tang, L.F. Chibotaru, D. Cui, An NCN-pincer ligand dysprosium single-ion magnet showing magnetic relaxation via the second excited state, *Scientific Reports*, 4 (2014).
- [20] S.K. Singh, T. Gupta, M. Shanmugam, G. Rajaraman, Unprecedented magnetic relaxation via the fourth excited state in low-coordinate lanthanide single-ion magnets: a theoretical perspective, *Chem. Commun.*, 50 (2014) 15513-15516.
- [21] J. Dreiser, R. Westerström, C. Piamonteze, F. Nolting, S. Rusponi, H. Brune, S. Yang, A. Popov, L. Dunsch, T. Greber, X-ray induced demagnetization of single-molecule magnets, *Appl. Phys. Lett.*, 105 (2014) 032411.
- [22] B. Donnio, E. Rivière, E. Terazzi, E. Voirin, C. Aronica, G. Chastanet, D. Luneau, G. Rogez, F. Scheurer, L. Joly, J.P. Kappler, J.L. Gallani, Magneto-optical interactions in single-molecule magnets: Low-temperature photon-induced demagnetization, *Solid State Sciences*, 12 (2010) 1307-1313.
- [23] A.L. Spek, Single-crystal structure validation with the program PLATON, *J. Appl. Crystallogr.*, 36 (2003) 7-13.
- [24] H.Q. Ye, Y. Peng, Z. Li, C.C. Wang, Y.X. Zheng, M. Motevalli, P.B. Wyatt, W.P. Gillin, I. Hernández, Effect of Fluorination on the Radiative Properties of Er<sup>3+</sup>+Organic Complexes: An Opto-Structural Correlation Study, *The Journal of Physical Chemistry C*, 117 (2013) 23970-23975.
- [25] W. Zheng, S.-J. Li, C.-H. Li, Y.-X. Zheng, X.-Z. You, Dramatic improvement in photostability of luminescent Eu(III) complexes with tetraphenylimidodiphosphinate ligand, *J. Lumin.*, 146 (2014) 544-549.
- [26] G. Mancino, A.J. Ferguson, A. Beeby, N.J. Long, T.S. Jones, Dramatic Increases in the Lifetime of the Er<sup>3+</sup> Ion in a Molecular Complex Using a Perfluorinated Imidodiphosphinate Sensitizing Ligand, *J. Am. Chem. Soc.*, 127 (2005) 524-525.
- [27] D. Aguilà, L.A. Barrios, V. Velasco, O. Roubeau, A. Repollés, P.J. Alonso, J. Sesé, S.J. Teat, F. Luis, G. Aromí, Heterodimetallic [LnLn'] Lanthanide Complexes: Toward a Chemical Design of Two-Qubit Molecular Spin Quantum Gates, *J. Am. Chem. Soc.*, 136 (2014) 14215-14222.
- [28] N. Ishikawa, M. Sugita, T. Ishikawa, S.-y. Koshihara, Y. Kaizu, Mononuclear Lanthanide Complexes with a Long Magnetization Relaxation Time at High Temperatures: A New Category of Magnets at the Single-Molecular Level, *The Journal of Physical Chemistry B*, 108 (2004) 11265-11271.
- [29] M.A. Antunes, L.C.J. Pereira, I.C. Santos, M. Mazzanti, J. Marçalo, M. Almeida, [U(TpMe<sub>2</sub>)<sub>2</sub>(bipy)]<sup>+</sup>: A Cationic Uranium(III) Complex with Single-Molecule-Magnet Behavior, *Inorg. Chem.*, 50 (2011) 9915-9917.
- [30] J.T. Coutinho, M.A. Antunes, L.C.J. Pereira, H. Bolvin, J. Marçalo, M. Mazzanti, M. Almeida, Single-ion magnet behaviour in [U(TpMe<sub>2</sub>)<sub>2</sub>I], *Dalton Trans.*, 41 (2012) 13568.
- [31] K.S. Cole, R.H. Cole, Dispersion and Absorption in Dielectrics I. Alternating Current Characteristics, *J. Chem. Phys.*, 9 (1941) 341.
- [32] S.M.J. Aubin, Z. Sun, L. Pardi, J. Krzystek, K. Folting, L.-C. Brunel, A.L. Rheingold, G. Christou, D.N. Hendrickson, Reduced Anionic Mn<sup>12</sup>Molecules with Half-Integer Ground States as Single-Molecule Magnets, *Inorg. Chem.*, 38 (1999) 5329-5340.
- [33] M. Bal, J.R. Friedman, E.M. Rumberger, S. Shah, D.N. Hendrickson, N. Avraham, Y. Myasoedov, H. Shtrikman, E. Zeldov, Photon-induced magnetization changes in single-molecule magnets (invited), *J. Appl. Phys.*, 99 (2006) 08D103.
- [34] W.H. Harman, T.D. Harris, D.E. Freedman, H. Fong, A. Chang, J.D. Rinehart, A. Ozarowski, M.T. Sougrati, F. Grandjean, G.J. Long, J.R. Long, C.J. Chang, Slow Magnetic Relaxation in a Family of Trigonal Pyramidal Iron(II) Pyrrolide Complexes, *J. Am. Chem. Soc.*, 132 (2010) 18115-18126.

[35] X.-L. Wang, L.-C. Li, D.-Z. Liao, Slow Magnetic Relaxation in Lanthanide Complexes with Chelating Nitronyl Nitroxide Radical, *Inorg. Chem.*, 49 (2010) 4735-4737.